Iran J Sci Technol Trans Civ Eng
https://doi.org/10.1007/s40996-018-0122-3

RESEARCH PAPER

Evaluation of the Seismic Bearing Capacity of Shallow Foundations Located on the Two-Layered Clayey Soils

M. Jahani[1] · M. Oulapour[1] · A. Haghighi[1]

Received: 12 September 2016 / Accepted: 4 June 2018

Abstract
The seismic bearing capacity of shallow strip footings located on homogeneous soils is studied extensively. But the effect of building height and layering is not included in those studies. In this paper two-layered cohesive soils are studied along with building height effect. The formulation of the problem is derived by extending the limit equilibrium method developed by Merlos and Romo (J Soil Dyn Earthq Eng 26(2):103–114, 2006) for two-layered soils. A log-spiral potential failure surface is assumed, and the inertia forces are applied directly to the building and the failure block soil mass. The position of the failure surface is obtained by a minimization process for every earthquake shaking acceleration. Results show that the potential failure surface moves upward and its length shortens as the peak ground acceleration (PGA) increases, reducing the bearing capacity. Also, the effects of building height, PGA, ratio of cohesion of the layers and the thickness of the top layer on seismic bearing capacity factor (N_{ce}) are studied.

Keywords Two-layer soil · Cohesion ratio · Seismic bearing capacity · Limit equilibrium · Peak ground acceleration

1 Introduction

The most severe loading condition a foundation undergoes is what happens during an earthquake. Thus, the design of foundations in seismic areas needs special consideration compared to the static case. Some researchers have studied the seismic bearing capacity of shallow strip footings, either theoretically or experimentally. Three main approaches are followed in theoretical studies: *pseudo-static, pseudo-dynamic and full dynamic analysis*. In *pseudo-static* approach, horizontal and vertical accelerations are applied to the center of gravity of the structure or at the foundation level, and the problem is reduced to a static case of bearing capacity with inclined eccentric loads. In most of these solutions, the inertia of the soil mass is not included. In a *pseudo-dynamic* approach, the failure surface developed during dynamic condition is assumed to be similar to the one under static loading and the equation of motion is derived from the dynamic equilibrium conditions. In this context, the effect of the earthquake on supporting soil is included in the equilibrium equation. Also, the distribution of earthquake acceleration is included. The *full dynamic* approach is based on time-history analysis using numerical methods.

The majority of the earlier studies are analytic in the context of pseudo-static approach. These studies use several different solution methods such as limit equilibrium, stress characteristics, limit analysis and variational methods. The first studies performed in limit equilibrium context did not include the inertia force on soil (Triandafilidis 1965). Subsequent studies considered the seismic forces both on the structure and on the supporting soil mass (Sarma and Iossifelis 1990; Richards et al. 1993; Kumar and Kumar 2003; Tiznado and Paillao 2014). In most of these cases, the failure surface is assumed to be a constant log-spiral (Fig. 1), the focus of which is at the edge of the footing, which is not supported by the actual performance of foundations. Merlos and Romo (2006) presented a new method in which time-varying inertia forces are applied directly to the building. This method is capable of estimating vertical displacements and foundation tilting by integrating the angular moment equilibrium differential equation. The position of the failure surface was obtained

✉ M. Oulapour
oulapour_m@scu.ac.ir

[1] Department of Civil Engineering, Shahid Chamran University of Ahvaz, Ahvaz, Islamic Republic of Iran

Published online: 09 June 2018

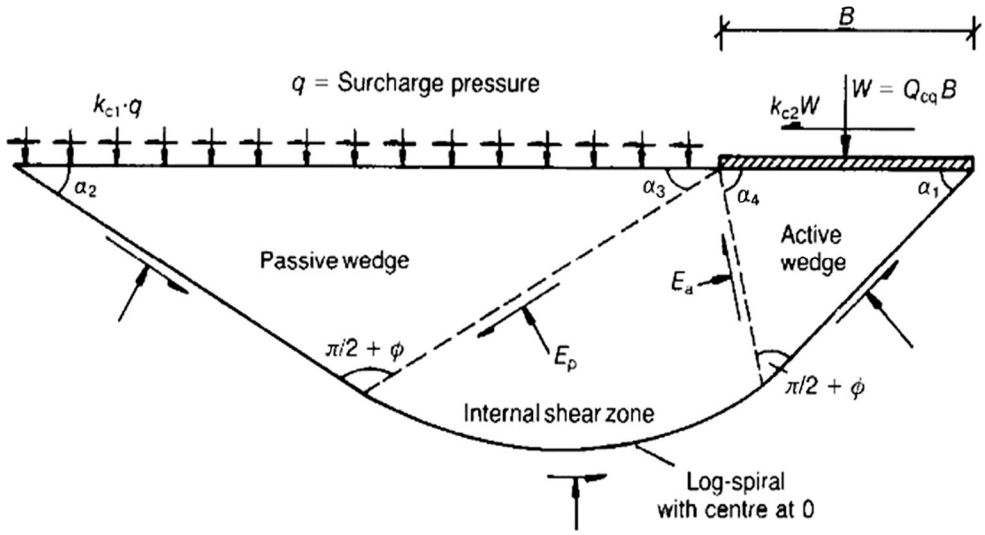

Fig. 1 Geometry of critical slip surface according to Sarma and Iossifelis (1990)

by a minimization process at every time increment. Results showed that under an earthquake loading the potential failure surface moves upward and its length shortens as the seismic accelerations increase, reducing the bearing capacity. Some researchers used the upper bound theorem of *limit state analysis* (Richards et al. 1993; Dormieux and Pecker 1995; Paolucci and Pecker 1997; Soubra 1999; Ghazavi and Parsapajouh 2006) to study the problem in a more rigorous way. The shear resistance of the soil mass above the footing level has not been incorporated in the previous analyses. Using upper bound theorem and including this shear resistance Kumar and Ghosh (2006) provided the values of the seismic bearing capacity factors for footing embedded on the sloping ground surface. Farzaneh et al. (2013) developed a rigorous lower bound solution using finite elements modified by extension elements which are used to extend the stress field into a semi-infinite domain. Using the homogenization technique and stress characteristics line method Keshavarz et al. (2011) modeled the seismic behavior of reinforced soil and calculated the pseudo-static earthquake coefficients. Soubra and Regenass (1992) used variational method, in which equilibrium and Mohr–Coulomb equations are the constraint functions and the bearing capacity function is minimized. This method is in good compatibility with observations of slip surface. Various numerical methods were applied utilizing realistic constitutive equations and accounting for earthquake characteristics including finite difference method (Kholdebarin et al. 2008), discrete element method (Majidi and Mirghasemi 2008) and finite element method (Shafiee and Jahanandish 2010; Elia and Rouainia 2014). Shafiee and Jahanandish (2010) used the finite element method for a wide range of friction angles and seismic coefficients, and compared to available solutions in the literature, the results showed that the soil inertia does not have any significant impact on the seismic bearing capacity. Also, many experimental studies are performed on small-scale models, among which Vesic et al. (1965), Das and Maji (1994), Boulanger and Idriss (2007) and Castelli and Lentini (2012) are notable. Using high-speed video, PIV and photogrammetry, Knappett et al. (2006) observed that the failure mechanism is similar to the surface assumed in the static case. It was observed that the failure mechanism changes during each cycle of the earthquake and as the earthquake PGA is increased the rotation center moves from the foundation corner toward its center.

The previous studies assume a homogenous and isotropic soil. Also, the effect of building is not included directly. In this study, the Merlos–Romo's approach is modified and used to include both soil layering and building effects in calculating the seismic bearing capacity of the foundations on cohesive soils. The effects of structure height, PGA, the ratio of cohesion of layers and the thickness of the first layer are studied.

2 Method of Analysis

Pseudo-static approach and limit equilibrium method are utilized for the calculation of seismic bearing capacity factors of two-layered cohesive soil. The soil in each layer is assumed to be homogeneous and isotropic. The soil is assumed as rigid-perfect-plastic material satisfying the Mohr–Coulomb failure criterion. The values of soil parameters, cohesion c and density of soil γ, are assumed to stay constant during an earthquake. Uniform seismic accelerations are assumed in the domain under

consideration. The horizontal seismic accelerations are considered both on the foundation and within the soil mass beneath the foundation seismic. Also, it is assumed that for seismic loading the failure surface changes in shape, length and depth depending on the horizontal acceleration applied to the system. This assumption improves the results.

2.1 Formulation of the Problem

According to D'Alembert's principle, an inertia force, F_{he}, is developed in opposite direction of the action of seismic force when the soil mass beneath the foundation moves due to earthquake loading and a logarithmic spiral potential failure surface is formed as shown in Fig. 2. The governing equations of the system are developed by considering the rotational equilibrium of the acting and resisting moments on the spiral center, 0. The acting forces include the building weight, W_e; the weight of the surrounding soil, W_{sa}; and the weight of the rotating soil mass, W_s.

When the acting moments exceed the resisting moments, the failure surface develops, and the system starts rotating as shown in Fig. 3a, where ψ is the rotation angle about the vertical line. Also, the dimensions of the building are given by width, B, height, H_e, foundation depth, D_f, and center of gravity, H_{eq}. Its length, B1, and coordinates of center of rotation x_{gi} and y_{gi} present the geometry of failure surface with α and β angles defining the log-spiral shape.

The D'Alembert's inertial force, F_{he}, is equal to:

$$F_{he} = m_e a_e = \frac{qBL}{g} a_e, \tag{1}$$

where m_e is the mass of the structure and a_e is the applied acceleration at the mass center of gravity and q is the pressure inserted by the structure on the foundation due to its weight. The horizontal and vertical distances of log-spiral center with respect to the point of application of horizontal earthquake force, x_d and y_d, can be calculated as:

$$x_d = \frac{B}{2} - x_{gi} = \frac{B - 2x_{gi}}{2} \tag{2}$$

$$y_d = H_{eq} - y_{gi}, \tag{3}$$

where x_{gi} and y_{gi} are the coordinates of the center of log-spiral with respect to the edge 1 of the building and H_{eq} is the height of the point of application of earthquake with respect to foundation edge, as shown in Fig. 3b.

2.1.1 Driving Moments

The driving moments include the one due to the weight of the structure and the one due to earthquake and rotation of the structure. The driving moment due to the weight of the structure is:

$$M_{awe} = W_e x_d = qBL\left(\frac{B - 2x_{gi}}{2}\right). \tag{4}$$

The driving moment due to the horizontal force of earthquake is calculated as follows:

$$M_{afh} = F_{he} y_d = \frac{qBL}{g} a_e y_d. \tag{5}$$

The driving moment due to the tilting of the structure under the static service loads is:

$$M_{aie} = W_e H_{eq} \psi = qBLH_{eq}\psi, \tag{6}$$

where ψ is the clockwise tilt angle as shown in Fig. 3. In this study it is assumed that the initial tilt of the structure is negligible.

2.1.2 Resisting Moments

The equation of log-spiral failure surface is:

$$r = r_0 e^{\theta \tan \varphi}, \tag{7}$$

in which r is equal to r_0 if θ is equal to zero. Also, it can be calculated as:

$$r_0 = \frac{r_1}{e^{\beta \cdot \tan \varphi}}, \tag{8}$$

where r_1 is the distance between the rotation center and building edge 2 and β is the angular between r_1 and r_0. For practical problems, it is necessary to study the layered soils. Extending the Richards' formulation, Ghazavi and Parsapajouh (2006) studied the two-layered sandy soils. But the two-layered clayey soils were not studied earlier.

Assuming a layered undrained clayey soil with zero internal friction angle ($\phi = 0$) the failure mechanism

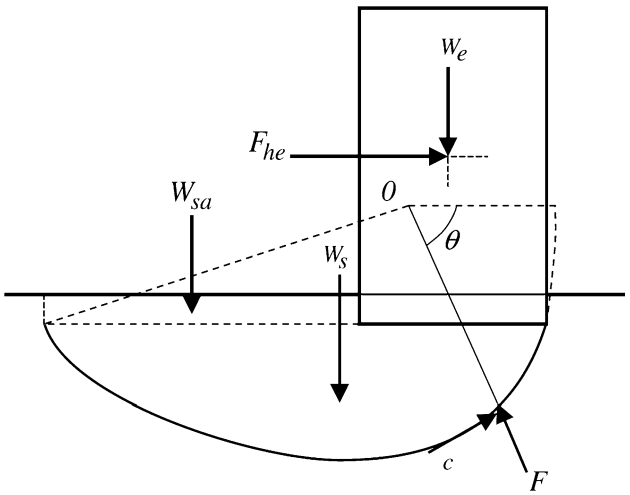

Fig. 2 Geometry of critical slip surface

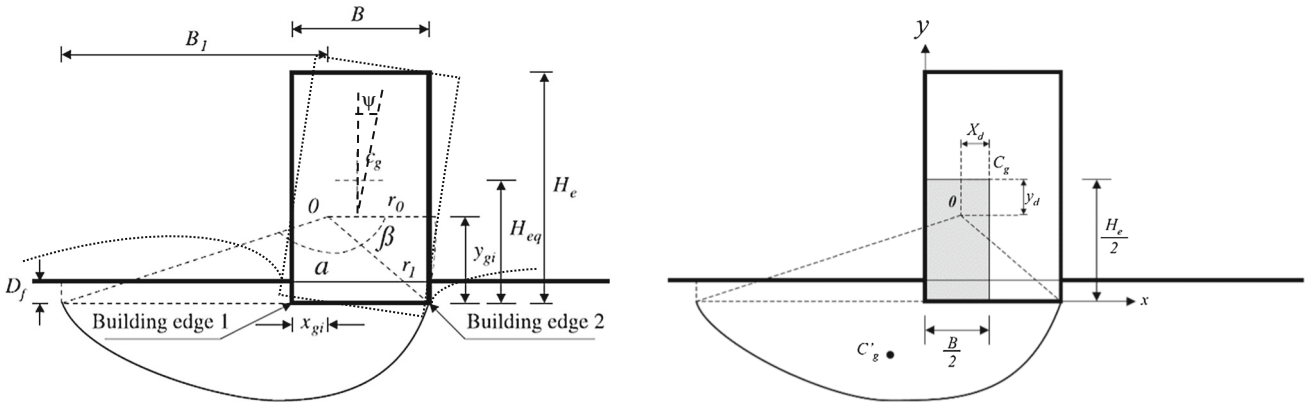

(a) Geometric parameters of the soil-building system **(b)** Region of the center of failure surface

Fig. 3 **a** Geometric parameters of the soil–building system; **b** region of the center of failure surface

degenerates to a circular arc, the center of which is to be determined through minimization of bearing capacity.

The equation of the circle is written as:

$$r = r_0, \tag{9}$$

in which r_0 is the radius of failure surface. The geometric and mechanical properties are presented in Fig. 4. The necessary condition for the failure to pass through the second layer is:

$$(r_0 - y_{gi}) \geq (H_1 - D_f), \tag{10}$$

in which H_1 is the thickness of the upper layer.

2.1.3 Two-Layered Soil

Considering the geometry of two-layered soil problem, if the foundation is seated in the first layer, $D_f < H_1$, the resisting moment due to cohesion can be written as:

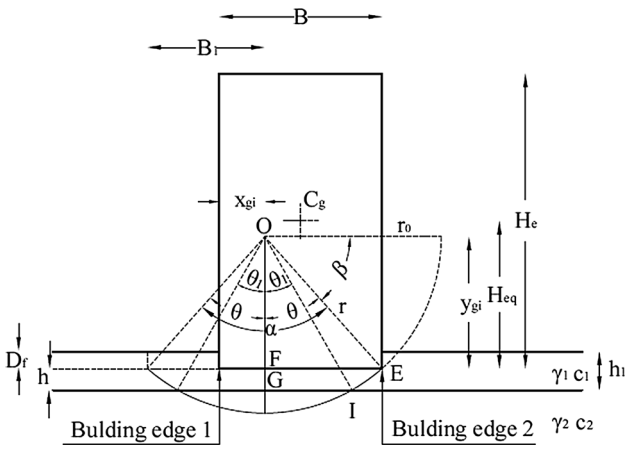

Fig. 4 Geometric and mechanical parameters of two-layered soil–building system

$$M_{rsf} = 2\left(c_1 r_0^2 L(\theta - \theta_1) + c_2 r_0^2 L\theta_1\right), \tag{11}$$

in which c_1 and c_2 are the cohesions of upper and lower layers, respectively. In OFE triangle it is evident that:

$$\cos\theta = \frac{y_{gi}}{r}. \tag{12}$$

Also, in OIG triangle:

$$\cos\theta_1 = \frac{y_{gi} + h}{r}. \tag{13}$$

The resisting moment due to internal friction of the soil is negligible. However, the resisting moment due to the weight of the surrounding the foundation can be calculated as:

$$M_{rsa} = \frac{\gamma_1 D_f L}{2}\left(B_1^2 - x_{gi}^2\right), \tag{14}$$

where γ_1 is the unit weight of the upper layer. In case that the failure surface is complete in the first upper layer, the condition presented in Eq. (10), the problem is reduced to a single clayey layer.

2.1.4 Seismic Bearing Capacity

At limit equilibrium the resisting moments and driving moments are equal. The seismic bearing capacity is derived by equating these two:

$$q_{ue} = \frac{\sum M_r = M_{ras} + M_{rsf}}{BL\left[x_d + \frac{|a_e|}{g} y_d\right]}, \tag{15}$$

where x_d and y_d are the coordinates of the center of gravity of the failure surface in the minimization region as shown in Fig. 3b. Using Eqs. (13) and (17) for moments, one can reach:

$$q_{ue} = \frac{\frac{\gamma_1 D_f}{2}\left(B_1^2 - x_{gi}^2\right) + 2\left(c_1 r_0^2(\theta_1 - \theta_2) + c_2 r_0^2 \theta_1\right)}{B\left[x_d + \frac{|a_{max}|}{g} y_d\right]}. \quad (16)$$

In this study the seismic bearing capacity is not constant and varies due to changes of the coordinates of the center of rotation and the extent of failure surface (Merlos and Romo 2006). It is clearly evident that earthquake acceleration has an inverse relation with the seismic bearing capacity. Therefore, the ultimate bearing capacity corresponds to peak ground accelerations. Assuming a peak ground acceleration, an optimization process is conducted in order to minimize the surcharge, which is calculated by Eq. (16) and considered as the ultimate bearing capacity at that specific horizontal acceleration. Also, the corresponding failure surface is considered as the critical surface. This is performed by using a computer program which changes the center of failure surface in the lower half of the structure for all points. Any point not in the shaded rectangular area in Fig. 4b, used as the center of failure surface, will give a higher bearing capacity, which is not on the safe side.

The results of calculations can be presented in a series of the non-dimensional format of graphs. The general non-dimensional form is given in (17):

$$\frac{q_{ue}}{c_1} = F\left(\frac{H_e}{B}, \frac{H_1}{B}, \frac{\gamma_1}{\gamma_2}, \frac{D_f}{B}, \frac{C_1}{C_2}, \frac{a_{max}}{g}\right), \quad (17)$$

where F denotes the function of seismic bearing capacity. In case of cohesive soils ($\phi = 0$) this equation reduces to:

$$N_{ce} = \frac{q_{ue}}{c_1}. \quad (18)$$

3 Results and Discussion

3.1 The Homogenous Soil

A homogenous soil foundation is modeled by assuming equal cohesion for both layers of the soil.

3.1.1 Comparison with Other Researches

The majority of researches in seismic bearing capacity are related to granular soils, and the results on cohesive soils are limited. Also, the effect of building height and layered soils is not studied in any previous research. In Fig. 5, available research and this method are compared for homogenous soils. The effect of building height is not included in other methods, such as Askari et al. (2005) and Kumar and Mohan Rao (2002). At low building heights the results are very close. This verifies the method used in this study. But a notable reduction in bearing capacity is predicted as the building height is increased. Also, the reduction is downsized as the peak acceleration is increased. This shows that ignoring the impact of building height can lead to an unsafe design.

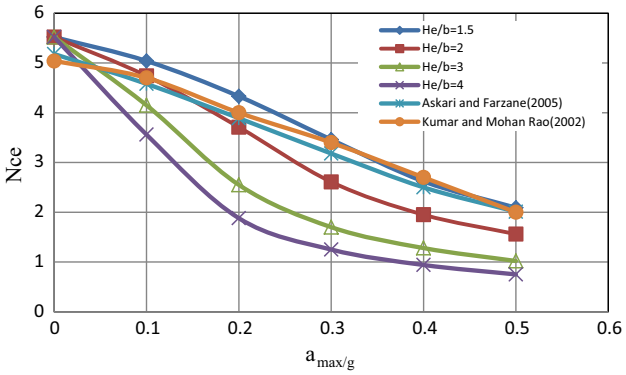

Fig. 5 Comparison of building height with other researches in homogeneous soils

3.1.2 The Effect of Building Height

The results of calculations for the case of buildings of different heights in a homogenous soil are presented in Fig. 6. It is evident that increasing the height of the structure reduces the seismic bearing capacity at any specific PGA. Similarly, increasing the PGA of earthquake reduces the seismic bearing capacity.

3.1.3 The Effect of Building Embedment

The effect of foundation embedment depth (D_f), for a wide range of building heights and foundation embedments and widths, is presented in Fig. 7. This shows that at similar conditions of building height, H_e, and foundation width, B, the foundation depth has a negligible effect on the seismic bearing capacity factor, N_{ce}.

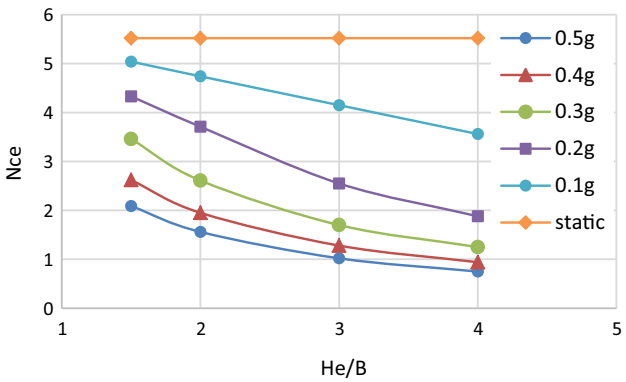

Fig. 6 Effect of building height on seismic bearing capacity in homogeneous soils

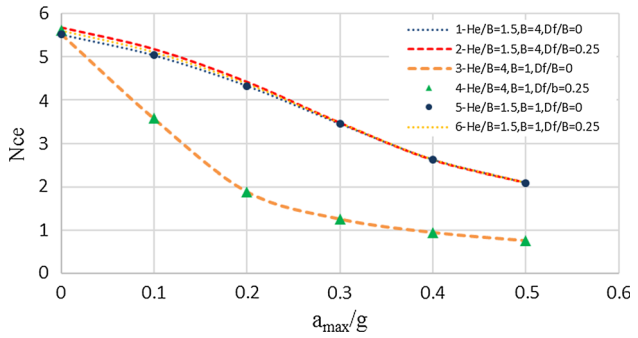

Fig. 7 Effect of building embedment on seismic bearing capacity in homogeneous soils

3.2 Two-Layered Soil

The extended formulation was used for reviewing the effect of a few influential parameters on the seismic bearing capacity. These parameters are usually ignored in such studies. The results are calculated for a broad range of values of different parameters involved, and only a few are presented in the following. Due to number and complexity of the problem and interaction of the parameters, the results presented in each part are for some practical values.

3.2.1 The Effect of Building Height and PGA

Figure 8 presents the effect of the height of the structure and PGA on the seismic bearing capacity for a variety of top layer thicknesses and the ratio of cohesion of the layers. As expected, increase in the height of the structure and PGA reduces the seismic bearing capacity. Also, for a certain thickness-to-width ratio (H_1/B) and cohesion ratio (C_1/C_2), the coefficient N_{CE} reduces to some limit as the building height is increased. This can be due to the fact that in those cases the failure mechanism becomes shallow and locates in the top layer. Therefore, it is less affected by the cohesion of the lower layer. Furthermore, as the height of the structure is increased the effect of PGA becomes more prominent, as the failure mechanism becomes shallower at lower PGA. It is interesting that at $C_1/C_2 < 1$, the coefficient N_{CE} is less than that of corresponding values for lower thickness ratio, H_1/B. However, in cases of $C_1/C_2 > 1$, the coefficient N_{CE} becomes higher than that of corresponding values for higher thickness ratio, H_1/B. This issue is due to the penetration of failure surface into the lower layer. When the top layer is thicker, its penetration is less into the lower stronger layer. It is found that at a certain height-to-width ratio, (H_e/B), and top layer thickness-to-width ratio, (H_1/B), increasing PGA drives the failure mechanism up and increases the effect of the upper layer. Also, the results compare well with the experimental results presented in Vesic et al. (1965) and Kumar and Mohan Rao (2002).

3.2.2 The Effect of the Ratio of Cohesions of the Layers

As the ratio of cohesion has a complex effect on the seismic bearing capacity ratio, as presented in Fig. 9, for a certain configuration and PGA, three features are encountered: initial constant part, quadratic decreasing part and final asymptotic part. The general trend is that as the cohesion ratio increases the failure surface penetrates more in the lower layer and, on the contrary, it becomes shallower as the ratio reduces down to about 1. At lower values of cohesion ratio, the failure surface remains in the upper layer. Therefore, the cohesion of the lower layer has no effect on the results. At high cohesion ratios as the failure surface penetrates deep into the lower layer, the effect of cohesion of upper layer has a very low effect on the results. Meanwhile, at intermediate cohesion ratios, the reduction trend is quadratic.

3.2.3 The Effect of the Thickness of the Top Layer

Considering the results presented in Fig. 10, it is concluded that increasing the thickness of the top layer decreases the influence of the lower layer. In case the ratio of thickness to width of the structure equals 1, the seismic bearing capacity ratio becomes constant as the whole failure mechanism locates in the top layer. The constant value depends on other effective parameters. Also, for a specific PGA and height-to-width ratio of the structure, the seismic coefficient ratio increases as the thickness of the top layer is increased if the top layer is stronger, $C_1/C_2 > 1$. If the top layer is weaker than the lower layer, $C_1/C_2 < 1$, and its thickness is enough, $H_1/B > 0.5$, the seismic coefficient becomes constant regardless of the cohesion ratio, C_1/C_2, as the failure surface does not penetrate into the lower layer.

3.2.4 The Effect of the Building Embedment

The failure mechanism is assumed to extend only to the foundation level, and the soil above the foundation depth is assumed only as a surcharge. Therefore, if the foundation depth is greater than the thickness of the top layer, the problem would reduce to a single-layer case. Figure 11 presents the results for a broad range of data showing the effect of building embedment. The trend for other data is very similar. As seen, at a certain thickness of the top layer, H_1/B, increasing the foundation depth, D_f/B, will increase the effect of the lower layer as the failure mechanism penetrates more in the lower layer. If the top layer is weaker, $C_1/C_2 < 1$, then the seismic bearing capacity

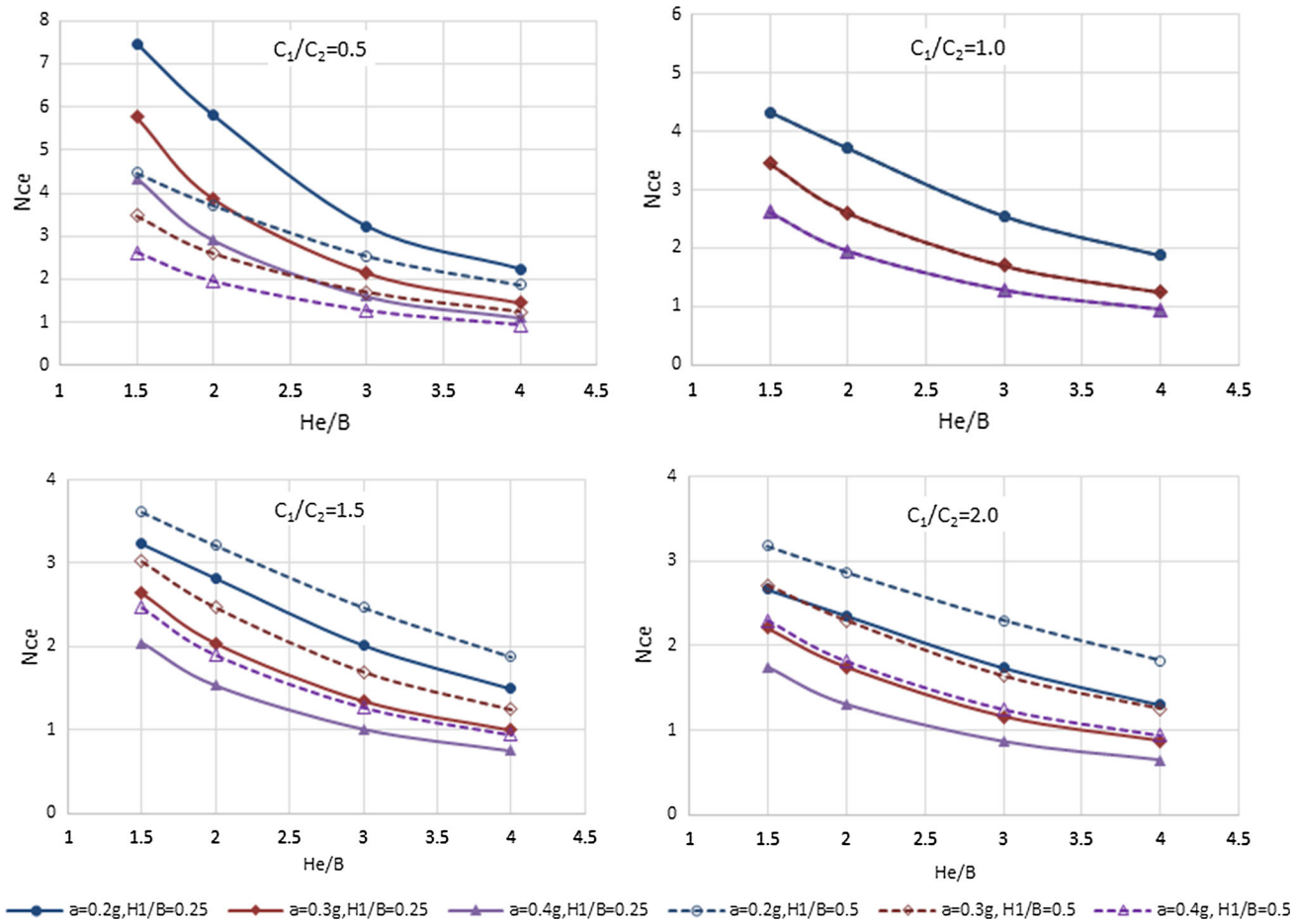

Fig. 8 Effect of building height and PGA on seismic bearing capacity in two-layered soils

factor, N_{ce}, will increase. However, if the top layer is stronger, $C_1/C_2 > 1$, the seismic bearing capacity factor, N_{ce}, will decrease. Also, if both H_1/B and D_f/B increase equally then the seismic factor increases only equal to increase in γD_f. In this study, the results of the $D_f/B = 0$ and $H_1/B = 0.5$ are very similar to the results of $D_f/B = 0.25$ and $H_1/B = 0.75$, as the increase in γD_f is very small due to small foundation width assumed for simulations. Since both the higher buildings, higher H_e/B, and higher earthquake PGA, higher $a\max/g$, drive the failure mechanism upward, the difference between a shallower foundation and deeper one will reduce as these are increased.

4 Conclusions

Using the limit equilibrium method and pseudo-static method of analysis, an extension of Merlos and Romo model is developed for considering the effect of soil layering and height-to-width ratio of building on the seismic bearing capacity of shallow strip foundations. These were not considered in earlier studies. The material is assumed to be rigid-perfect-plastic. The model was verified by comparing with the results of homogeneous soils. Also, the effects of some effective parameters on the seismic bearing capacity factor are studied and compared to experimental results. The results emphasize that the bearing capacity is reduced mainly due to the horizontal force of earthquake under seismic loading, which drives the failure surface upward. The results, also, clearly show that the failure surface position and size and the seismic safety of the foundations depend on the acceleration magnitudes developed throughout the seismic event as shown in Figs. 7, 8 and 9. This is supported by the experiments presented in Boulanger and Idriss (2007), Knappett et al. (2006) and Vesic et al. (1965). In both cases of homogeneous or two-layered soils, increasing the PGA of an earthquake or the height of the structure reduces the seismic bearing capacity factor. The cohesion ratio has a complex effect on the seismic bearing capacity factor. In general, the failure surface tends toward the weaker layer. The failure surface would confine in the top layer if this layer is weaker, while if the stronger layer is on the top, the failure surface would

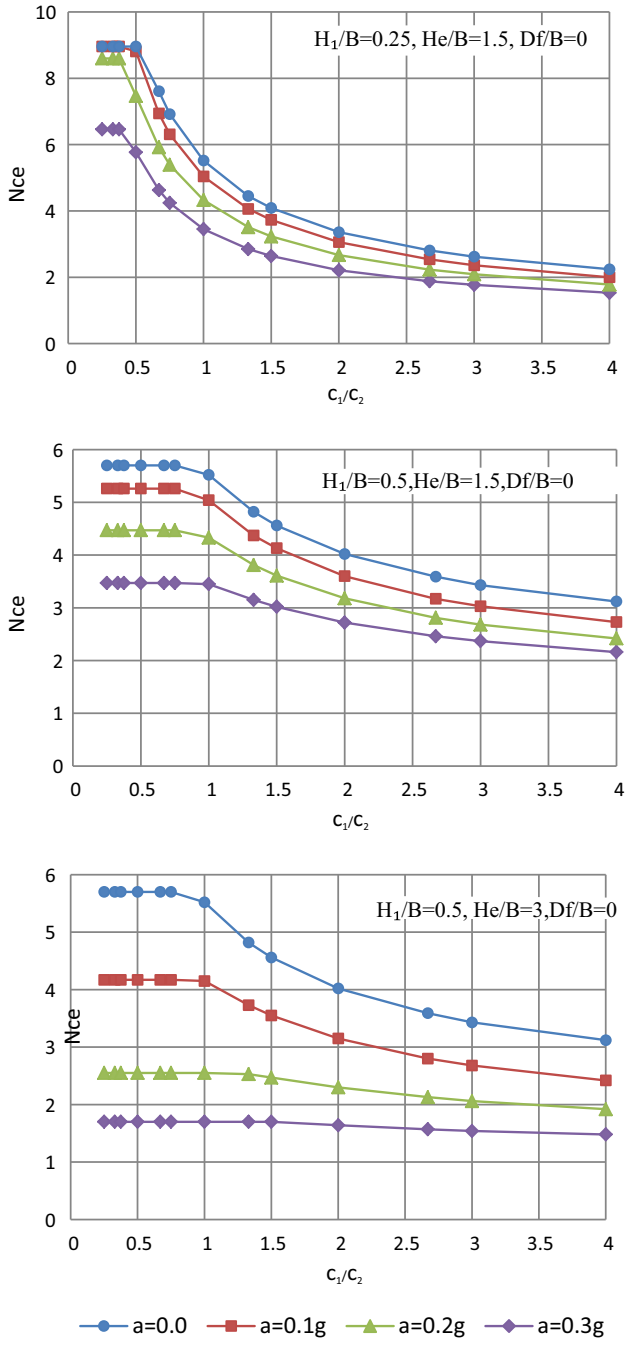

Fig. 9 Effect of cohesion ratio on seismic bearing capacity in two-layered soils

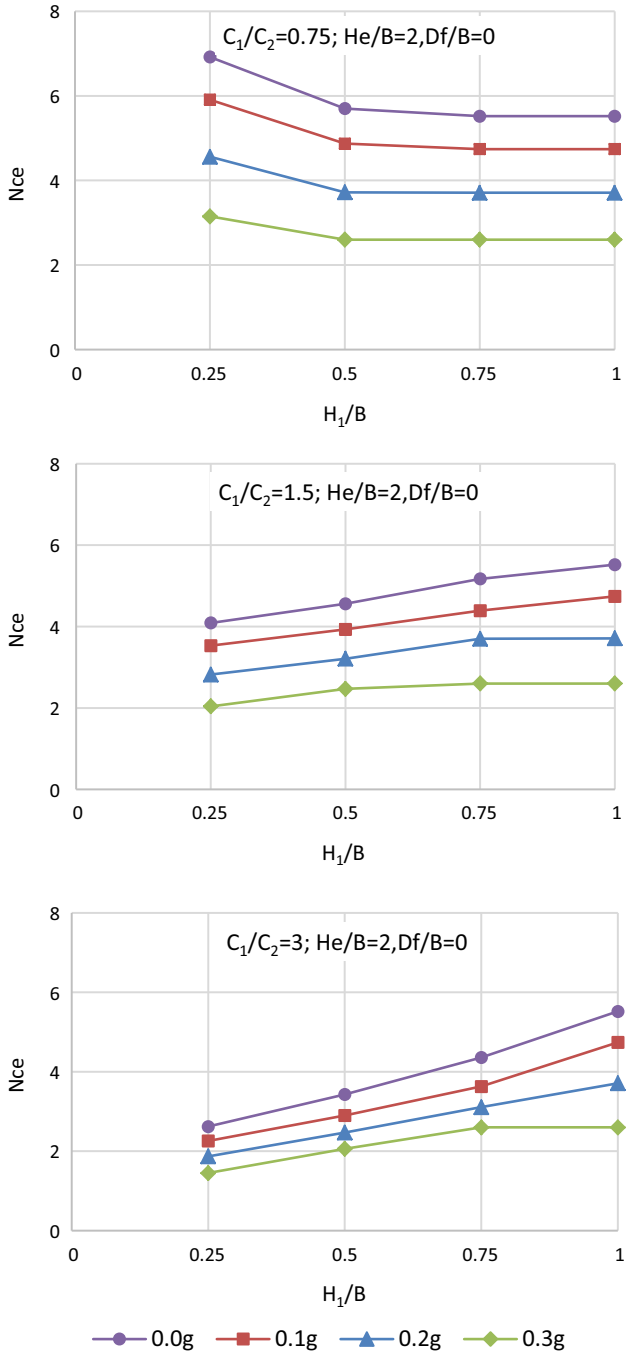

Fig. 10 Effect of top layer thickness on seismic bearing capacity in two-layered soils

penetrate deep into the lower weak layer. If the thickness of the top layer, H_1, is greater than 0.5B, then the lower layer is not contributing, and the bearing capacity factor remains constant if the top layer is weaker, while if the top layer is stronger, thicker top layers increase the bearing capacity factor as the contribution of lower weak layer reduces. Also, it was concluded that increasing the foundation depth, D_f/B, increases the effect of the lower layer as the failure mechanism penetrates more in the lower layer. A weak top layer increases the seismic bearing capacity factor, while a stronger top layer reduces it. If both the thickness and foundation depth ratios increase equally, the seismic bearing capacity factor remains constant.

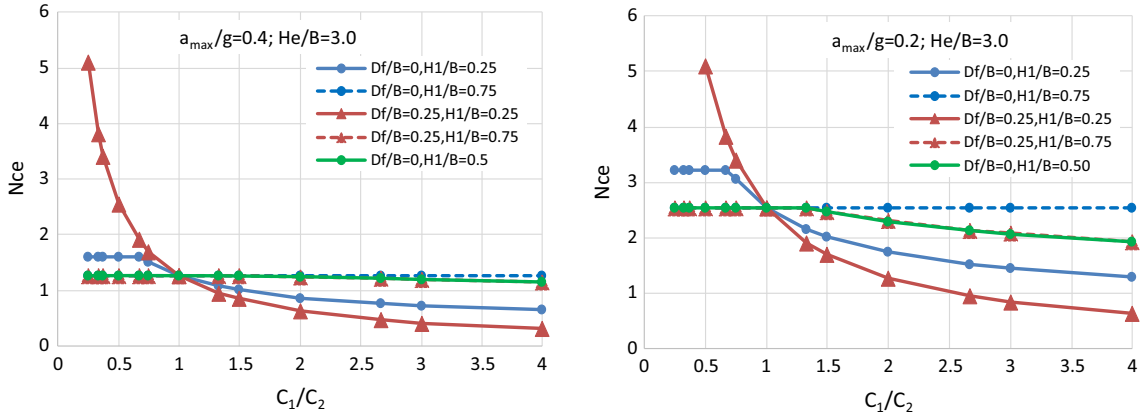

Fig. 11 Effect of foundation embedment on seismic bearing capacity in two-layered soils

References

Askari F, Farzaneh O, Mirabotalebi M (2005) Seismic bearing capacity of shallow foundation including the inertia force of soil. J Eng Fac Tehran Univ 39(3):319–327

Boulanger R, Idriss I (2007) Evaluation of cyclic softening in silts and clay. J Geotech Geoenviron Eng ASCE 133(6):641–652

Castelli F, Lentini V (2012) Evaluation of the bearing capacity of footings on slope. Int J Phys Model Geotech Eng 12(3):112–118

Das BM, Maji A (1994) Transient loading-related settlement of a square foundation on geogrid-reinforced sand. J Geotech Geolog Eng 12(4):241–251

Dormieux L, Pecker A (1995) Seismic bearing capacity of foundation on cohesionless soil. J Geotech Eng 121(3):300–303. https://doi.org/10.1061/(ASCE)0733-9410

Elia G, Rouainia M (2014) Performance evaluation of a shallow foundation built on structured clays under seismic loading. Bull Earthq Eng 12(4):1537–1561

Farzaneh O, Mofidi J, Askari F (2013) Seismic bearing capacity of strip footings near cohesive slopes using lower bound limit analysis. In: Proceedings of the 18th international conference on soil mechanics and geotechnical engineering, Paris, pp 1467–1470

Ghazavi M, Parsapajouh A (2006) A simple method for calculating the effect of soil saturation on seismic bearing capacity of shallow foundations. In: Proceedings 7th international conference on civil engineering, Tarbiat Moddaress University of Tehran, I.R.Iran, pp 1467–1475

Keshavarz A, Jahanandish M, Ghahramani A (2011) Seismic bearing capacity analysis of reinforced soils by the method of stress characteristics. IJST Trans Civ Eng 35(C2):185–197

Kholdebarin AR, Massumi A, Davoodi M (2008) Influence of soil improvement on seismic bearing capacity of shallow foundations. In: Proceedings 14th world conference on earthquake engineering, Beijing, China, pp 560–569

Knappett JA, Haigh SK, Madabhushi SPG (2006) Mechanisms of failure for shallow foundations under earthquake loading. J Soil Dyn Earthq Eng 26(1):91–102

Kumar J, Ghosh P (2006) Seismic bearing capacity for embedded footings on sloping ground. Géotechnique 56(2):133–140

Kumar J, Kumar N (2003) Seismic bearing capacity of rough footings on slopes using limit equilibrium. Géotechnique 53(3):363–369

Kumar J, Mohan Rao VBK (2002) Seismic bearing capacity factors for spread foundations. Geotechnique 52(2):79–88

Majidi R, Mirghasemi AA (2008) Seismic 3D bearing capacity of shallow foundations. Iran J Sci Technol Tran B Eng 32(B2):107–124

Merlos J, Romo MP (2006) Fluctuant bearing capacity of shallow foundations during earthquakes. J Soil Dyn Earthq Eng 26(2):103–114

Paolucci R, Pecker A (1997) Seismic bearing capacity of shallow strip foundations on dry soils. Soils Found 37(3):95–105

Richards R, Elms DG, Budhu M (1993) Seismic bearing capacity and settlement of foundations. J Geotech Eng ASCE 119(4):662–674

Sarma SK, Iossifelis IS (1990) Seismic bearing capacity factors of shallow strip footings. Géotechnique 40(2):265–273

Shafiee AH, Jahanandish M (2010) Seismic bearing capacity factors for strip footings. In: Proceedings 5th National Congress on Civil Engineering, Ferdowsi University of Mashhad, Mashad, Iran, pp 1–8

Soubra AH (1999) Upper-bound solutions for bearing capacity of foundations. J Geotech Geoenviron Eng ASCE 125(1):59–68

Soubra AH, Regenass P (1992) Bearing capacity in seismic areas by a Variational approach. In: Pande GN, Pietruszczak S (eds) Proceedings of the fourth international symposium on numerical models in geomechanics, NUMOG IV, Swansea, Balkema, pp 421–429

Tiznado JC, Paillao VD (2014) Analysis of the seismic bearing capacity of shallow foundations. J Constr 13(2):40–48

Triandafilidis GE (1965) The dynamic response of continuous footing supported on cohesive soils. In: Proceedings of the 6th international conference on soil mechanics and foundation engineering, vol 2, pp 205–208

Vesic AS, Banks DC, Woodard JM (1965) An experimental study of dynamic bearing capacity of footings on sand. In: Proceedings of the 6th international conference on soil mechanics and foundation engineering, Montreal, Canada, vol 2, pp 209–213